ENGINEERING TRANSACTIONS • *Engng. Trans.* • **65**, 3, 499–511, 2017
Polish Academy of Sciences • Institute of Fundamental Technological Research (IPPT PAN)
National Engineering School of Metz (ENIM) • Poznan University of Technology

Research Paper

Strain Energy Method for Determining Dynamic Yield Stress in Taylor's Test

Edward WŁODARCZYK, Marcin SARZYŃSKI

Military University of Technology
Faculty of Mechatronics and Aviation
Sylwestra Kaliskiego 2, 00-908 Warszawa, Poland
e-mail: {edward.wlodarczyk, marcin.sarzynski}@wat.edu.pl

This paper presents a theoretical method for determining dynamic yield stress of metals. The method is based on conversion of the part initial kinetic energy of a metal rod striking a rigid target into the energy of elastic and plastic-strain deformation at selected period t_s. By means of this method, a theoretical simple algebraic formula has been derived for determining the dynamic yield stress of metals loaded by the Taylor direct impact experiment (Taylor DIE). This formula gives the results comparable with experimental data.

Key words: dynamic plasticity, dynamic yield stress, impact loading – Taylor's experiment.

1. Introduction

The Taylor DIE developed by Taylor [1] is a useful experiment for estimating material behaviour at high strain rates. The test is reproducible and reasonably economical after the initial investment has been made. This is why the Taylor test has been commonly employed in several studies [2–11] to determine dynamic yield stress of solids at the high strain rate. However, the current view is that Taylor's theory fails to provide reliable yield stress estimation, especially for the tests conducted at higher velocities. It ought to be taken into account that the theoretical model developed by Taylor is based on simplifications greatly deviating from the conventional dynamic plasticity theory.

For this reason, a lot of investigators correlate their results with sophisticated computer analyses that utilize several complex forms of constitutive equations. These programs can match the geometry of a post-test specimen with very high accuracy and provide very reliable estimates for material properties. The drawback is that these programs are expensive and often require a substantial amount of time to execute.

Simple engineering theories, such as that given by Taylor, are still recognised. Such theories frequently give investigators insight into the interaction of the physical parameters and their relationship to the outcome of the event. These interactions are difficult to ascertain from complex computer outputs. As a result, simple engineering theories often provide the basis for the design of experiments and are frequently used to refine the areas in which computing is to be done.

A new strain energy method for theoretical calculating dynamic yield stress of metals loaded by Taylor DIE is presented in this paper. By means of this method, a simple algebraic formula for estimating dynamic yield stress has been derived in a closed form. The derivation of the formula is based on a wave solution of the Taylor impact problem.

2. Formulation of the problem and assumptions

The considered homogeneous rod of initial dimensions: length L and cross-sectional area A impacts perpendicularly on the rigid target. Let x denote a Lagrangian coordinate aligned with the axis of the rod and having origin at the free end of the rod opposite to the striking one. The impact velocity of the rod is denoted by V_0. It is assumed that V_0 is sufficiently high to produce plastic strains in the rod. The characteristic of the rod material is described by an elastic-plastic model with linear strain hardening.

It has been proved both theoretically and experimentally [3, 10–12] that strain ε insignificantly decreases along the axis of the plastically deformed portion of the rod neighbouring the target during the Taylor DIE (Fig. 1). Therefore, the strain rate $d\varepsilon/dt$ in the initial plastically deformed part of such a loaded rod is very small and comparable with a quasistatic value. By contrast, at the final

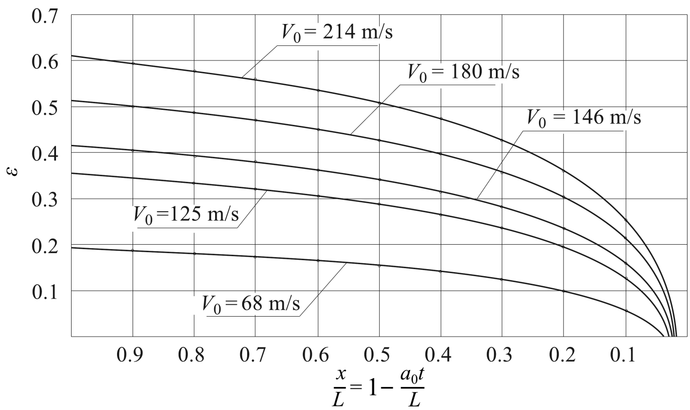

Fig. 1. Distributions of strain ε along the axis of the copper (Cu-ETP) rod deformed by the Taylor DIE [10].

stage of deformation of the rod portion, the strain rate intensively increases and reaches the value of 10^4 1/s and more (Fig. 2). Bearing in mind the above mentioned results of the performed investigations it has been assumed that the metal in the initial plastically deformed portion of the rod loaded by the Taylor DIE behaves as a rate-independent material, and is described by an elastic-plastic model with linear strain hardening (the Prandtl-Reuss model – Fig. 3).

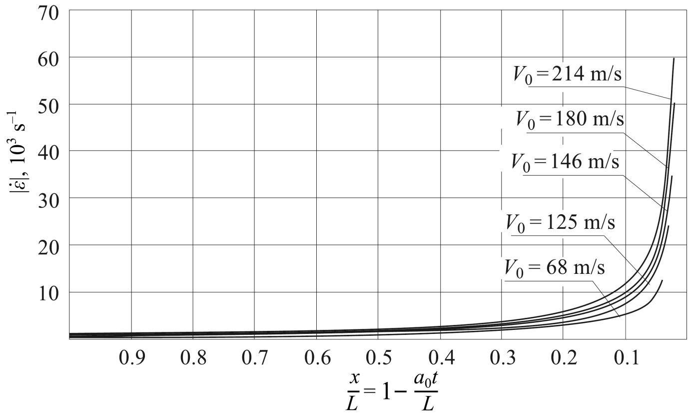

FIG. 2. Distributions of strain rate $|\dot{\varepsilon}| = \left|\frac{d\varepsilon}{dt}\right|$ along the axis of the copper (Cu-ETP) rod [10].

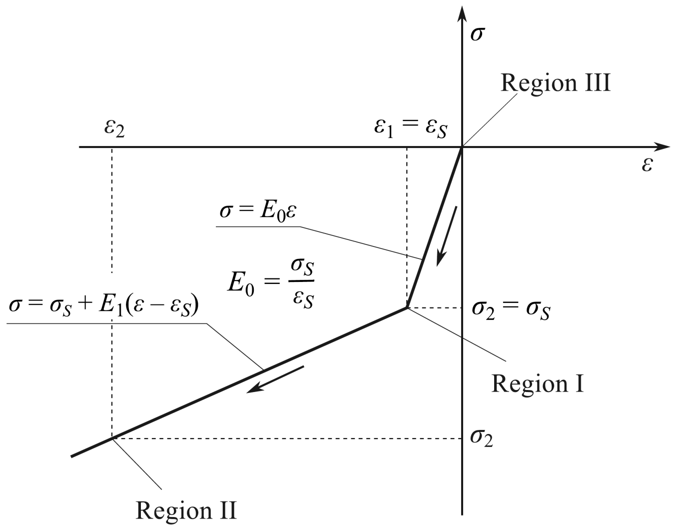

FIG. 3. Stresses and strains during loading.

The above formulated issue has been solved by means of the weak shock wave theory and is presented in monographs [13–15]. The fragment of this solution is applied in the following considerations.

3. Dynamics of the metal flat-ended circular rod perpendicularly striking a rigid flat target

At the moment when the rod strikes a rigid target two compression weak shock waves start to propagate in the rod away from the target. Firstly the elastic wave propagates at speed a_0 and is followed by the other plastic wave that propagates at speed a_1. The trajectories of these wave fronts are described by the equations: $x = L - a_0 t$ and $x = L - a_1 t$, respectively, on the plane $x0t$ (Fig. 4). The compression elastic wave reflects from the free end of the rod and propagates in the opposite direction as an elastic tension wave. This wave reduces the compression stress in the portion of the rod contained in the interval $0 \leq x \leq x_s$ (Fig. 4). When the front of the plastic wave and that of the reflected elastic wave meet in section S at instant t_s (Fig. 4) several outcomes are possible, depending on the magnitude of the impact velocity V_0, [13–15]. In Fig. 4, a scenario is presented when after the two wave fronts meet, the plastic wave does not propagate any further, and the elastic waves spread then from S in both directions.

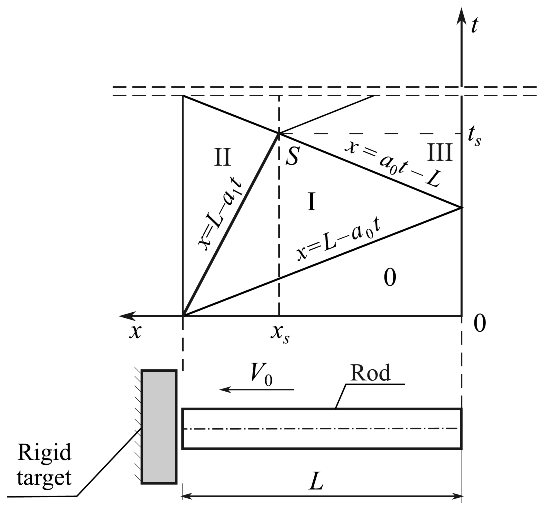

Fig. 4. Fragment of the configuration of trajectories of shock wave fronts on plane $x0t$.

As it can be seen in Fig. 4, the trajectories of the wave fronts divide the zone of the plane $x0t$, bounded by the values of the coordinate: $x = 0$ and $x = L$, into a series of regions.

Kinematic and dynamic conditions across the trajectories, completed by boundary conditions and a stress-strain relation (the Prandtl-Reuss model), determine the values of the parameters of the rod dynamics: stress – σ, strain – ε, and particle velocity – υ in separate regions, which can be found in [13–15] and are presented below:

- Region 0: $0 \le x \le L$, $0 \le t \le ((L-x)/a_0)$,

$$\upsilon_0(x,t) \equiv V_0, \qquad \sigma_0(x,t) \equiv 0, \qquad \varepsilon_0(x,t) \equiv 0. \tag{3.1}$$

- Region I: $0 \le x \le x_s$, $(L-x)/a_0 \le t \le (L+x)/a_0$,

$$x_s \le x \le L, \qquad (L-x)/a_0 \le t \le (L-x)/a_1,$$

$$x_s = \frac{a_0 - a_1}{a_0 + a_1} L,$$

$$\begin{gathered} \upsilon_1(x,t) \equiv V_0 + a_0\varepsilon_s, \qquad \sigma_1(x,t) \equiv \sigma_s, \qquad \varepsilon_1(x,t) \equiv \varepsilon_s, \\ \varepsilon_s < 0, \qquad \sigma_s = E_0\varepsilon_s < 0. \end{gathered} \tag{3.2}$$

- Region II: $x_s \le x \le L$, $(L-x)/a_1 \le t \le (L+x)/a_0$,

$$\begin{gathered} \upsilon_2(x,t) \equiv 0, \qquad \sigma_2(x,t) \equiv [(a_1/a_0) - 1]\,\sigma_s - \rho a_1 V_0, \\ \varepsilon_2(x,t) \equiv [(a_0/a_1) - 1]\,\varepsilon_s - (V_0/a_1). \end{gathered} \tag{3.3}$$

- Region III: $0 \le x \le x_s$, $(L+x)/a_0 \le t \le t_s$, $t_s = \frac{2L}{a_0+a_1}$,

$$\upsilon_3(x,t) \equiv V_0 + 2a_0\varepsilon_s, \qquad \sigma_3(x,t) \equiv 0, \qquad \varepsilon_3(x,t) \equiv 0, \qquad \varepsilon_s < 0. \tag{3.4}$$

According to the Prandtl-Reuss model for loading process:

$$\begin{aligned} &\sigma = E_0\varepsilon && \text{– for elastic strain,} \\ &\sigma = \sigma_s + E_1(\varepsilon - \varepsilon_s) && \text{– for plastic strain,} \end{aligned} \tag{3.5}$$

$$E_0 = \rho a_0^2, \qquad E_1 = \rho a_1^2, \tag{3.6}$$

where symbols: σ, ε, σ_s, ε_s, E_0, E_1, a_0, a_1, υ and ρ denote: engineering stress, total engineering strain, yield stress, engineering strain at yield stress, Young's modulus, linear plastic strain hardening modulus, velocity of propagation of the elastic wave front in Lagrangian coordinate, analogous velocity of propagation of the plastic wave front, and particle velocity and density of the rod material, respectively. A subscript in σ, ε and υ, in formulae (3.1)–(3.4) denotes the number of the region in which they are.

4. Derivation of the formula for determining dynamic yield stress

The formula for determining dynamic yield stress is based on the momentary energy balance of the rod portions which are created by the trajectories of the wave fronts. This balance ought to be performed at the suitable instant during the striking process. To simplify the description of the following considerations, this instant has been selected in such a way that all the trajectories of the wave fronts have a common point of the meeting (see Fig. 4 – point S). This condition is fulfilled by the following instant:

$$t_s = \frac{2L}{a_0 + a_1}. \tag{4.1}$$

In this case, in order to perform the momentary energy balance the energies in the rod portions contained in region II and region III at the instant t_s ought to be determined. Let h_2 denote the length of the plastically deformed part of the rod contained in region II at the moment t_s, which is defined by the formula:

$$h_2 = L - X_S(x_s, t_s), \tag{4.2}$$

where X_S $(x_s,\ t_s)$ denotes the Eulerian coordinate of point S at moment t_s.

From the values of the particle velocities υ_0 and υ_1 and the relationships determining boundaries of region 0 and region I it follows that

$$x_s = L - a_1 t_s = \frac{a_0 - a_1}{a_0 + a_1} L, \tag{4.3}$$

$$\begin{aligned} X_s = x_s + \frac{L - x_s}{a_0} V_0 + 2\frac{x_s}{a_0}\upsilon_1 &= \left(1 - \frac{V_0}{a_0} + 2\frac{V_0}{a_0} + 2\varepsilon_s\right) x_s + \frac{V_0}{a_0} L \\ &\approx \frac{a_0 - a_1 + 2V_0}{a_0 + a_1} L, \qquad 2\varepsilon_s \ll 1. \end{aligned} \tag{4.4}$$

From Eq. (4.2) and (4.4):

$$h_2 = \frac{2(a_1 - V_0)}{a_0 + a_1} L. \tag{4.5}$$

In turn the length of the rod portion contained in region III at moment t_s is determined by formula:

$$h_3 = L - (h_2 + X_k), \tag{4.6}$$

where X_k is displacement of the free rod end at instant t_s, i.e.

$$\begin{gathered} X_k = \frac{V_0}{a_0} L + \frac{\upsilon_3}{a_0} x_s = 2\left(\frac{V_0}{a_0 + a_1} + \frac{a_0 - a_1}{a_0 + a_1}\varepsilon_s\right) L \approx \frac{2V_0}{a_0 + a_1} L, \\ (a_0 - a_1)\,\varepsilon_s \ll V_0. \end{gathered} \tag{4.7}$$

Expressions (4.5), (4.6) and (4.7) result in:

$$h_3 = \frac{a_0 - a_1}{a_0 + a_1} L = x_s. \tag{4.8}$$

The balance of energy of the rod portions contained in region II and region III and initial kinetic energy of the whole rod at instant t_s can be written as

$$h_2 \Phi + \frac{1}{2} h_3 \rho v_3^2 = \frac{1}{2} L \rho V_0^2. \tag{4.9}$$

The conversion period of the initial kinetic energy of the rod into energy components of the rod portion contained in regions II and III lasts about a few μs. Therefore in order to facilitate the solution of issue under consideration, this process can be approximated as an adiabatic one and heat is therefore not included in the relationship (4.9).

The elastic – plastic energy per unit of volume Φ, in accordance with the Prandtl-Reuss model σ–ε (Fig. 3) for the loading process of the rod portion in region II is defined by the formula:

$$\Phi = \frac{\sigma_s \varepsilon_2}{2} + \frac{\sigma_2 (\varepsilon_2 - \varepsilon_s)}{2}. \tag{4.10}$$

In order to simplify a description of the following transformations the dimensionless quantities are introduced:

$$P = \frac{\sigma_s}{E_0} = \frac{\sigma_s}{\rho a_0^2} = \varepsilon_s, \qquad V = \frac{V_0}{a_0}, \qquad \alpha = \frac{a_1}{a_0}. \tag{4.11}$$

After substitution of relationship (3.3) into expression (4.10) and considering (4.11):

$$\Phi = \frac{E_0}{2} \left[2(1-\alpha)\varepsilon_s^2 + 2(\alpha - 1) V \varepsilon_s + V^2 \right]. \tag{4.12}$$

The energy of the plastic deformation contained in segment h_2 of the rod amounts to:

$$E_2 = \frac{1}{2} E_0 A L \left[\frac{4(\alpha - V)(1-\alpha)}{(\alpha+1)} \varepsilon_s^2 - \frac{4(\alpha - V)(1-\alpha)}{(\alpha+1)} V \varepsilon_s + 2 \frac{(\alpha - V)}{\alpha+1} V^2 \right]. \tag{4.13}$$

In turn, kinetic energy of portion h_3 of the rod is equal to:

$$E_3 = \frac{1}{2} h_3 A \rho v_3^2 = \frac{1}{2} E_0 A L \frac{1-\alpha}{1+\alpha} \left(4\varepsilon_s^2 + 4V\varepsilon_s + V^2 \right). \tag{4.14}$$

With expressions (4.13) and (4.14), Eq. (4.9) may be re-written as

$$P^2 + bP - c = 0, \tag{4.15}$$

where

$$b=\frac{1-\alpha+V}{1+\alpha-V}V, \qquad c=\frac{V^3}{2\,(1-\alpha)(1+\alpha-V)}. \tag{4.16}$$

From Eq. (4.15) and (4.16) it follows that

$$P=\frac{1}{2}\left\{-\frac{1-\alpha+V}{1+\alpha-V}+\left[\left(\frac{1-\alpha+V}{1+\alpha-V}\right)^2+\frac{2V}{(1-\alpha)(1+\alpha-V)}\right]^{1/2}\right\}V.$$

Accordingly, the dynamic yield stress is defined by an explicit algebraic formula:

$$\begin{aligned}|\sigma_{sd}|&=|PE_0|\\&=\frac{1}{2}\left\{-\frac{1-\alpha+V}{1+\alpha-V}+\left[\left(\frac{1-\alpha+V}{1+\alpha-V}\right)^2+\frac{2V}{(1-\alpha)(1+\alpha-V)}\right]^{1/2}\right\}VE_0.\end{aligned} \tag{4.17}$$

A simple Taylor formula for σ_{sd} has the following form [1]:

$$\sigma_{sd}=\frac{L-X}{2\,(L-L_1)\ln{(L/X)}}\rho V_0^2, \tag{4.18}$$

where L_1 is an overall length of the rod after the Taylor DIE, and X denotes the final length of the undeformed rod portion. This formula was derived by means of the momentum balance across the plastic wave front for rigid – ideal plastic material of the rod. For that reason, the formula (4.18) does not fulfil a dynamic condition across this wave front.

A comparison of the results obtained by the above mentioned formulae (4.17) and (4.18) is presented in the following section of the paper.

5. The results for the copper (Cu-ETP)

Homogeneously annealed (500°C, 1 h) copper (Cu-ETP) rods of the initial dimensions: length $L_0 = 0.048$ m and diameter $D_0 = 0.012$ m have been used in the Taylor DIE. The mechanical parameters of the copper rods are: density $\rho = 8900$ kg/m^3, the engineering static yield strength $R_{0.2} = 84$ MPa, Young's modulus $E_0 = 130$ GPa, the linear strain hardening modulus $E_1 = 1.1$ GPa, the speed of elastic wave propagation $a_0 = 3820$ m/s, and the speed of plastic wave propagation $a_1 = 350$ m/s. A static load-compression curve for the cylinder made of the Cu-ETP copper with a 0.01 m diameter and 0.01 m thickness is depicted in Fig. 5, where φ is the true (logarithmic) strain, and ε is nominal (engineering) strain; $\varepsilon = 1 - \exp(-\varphi)$.

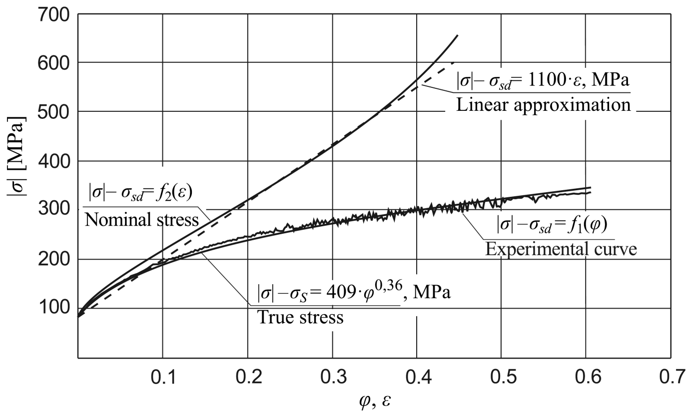

FIG. 5. A static load-compression curve for a cylinder made of copper (Cu-ETP) with a 0.01 m diameter and 0.01 m thickness.

Figure 5 shows that the static curve of the nominal values of the stress-strain within the scope $|\varepsilon| < 0.4$ can be approximated by means of a straight line namely $|\sigma| - \sigma_{sd} = 1100|\varepsilon|$ [MPa] (a dashed line in Fig. 5). An approximation error does not exceed several percent.

Cylindrical samples were driven by a light gas gun (Fig. 6) to some moderate values of the impact velocities (68 m/s $\leq V_0 \leq 214$ m/s), after which they struck perpendicularly on a flat rigid target. Pictures of the deformed rods after the Taylor DIE are depicted in Fig. 7.

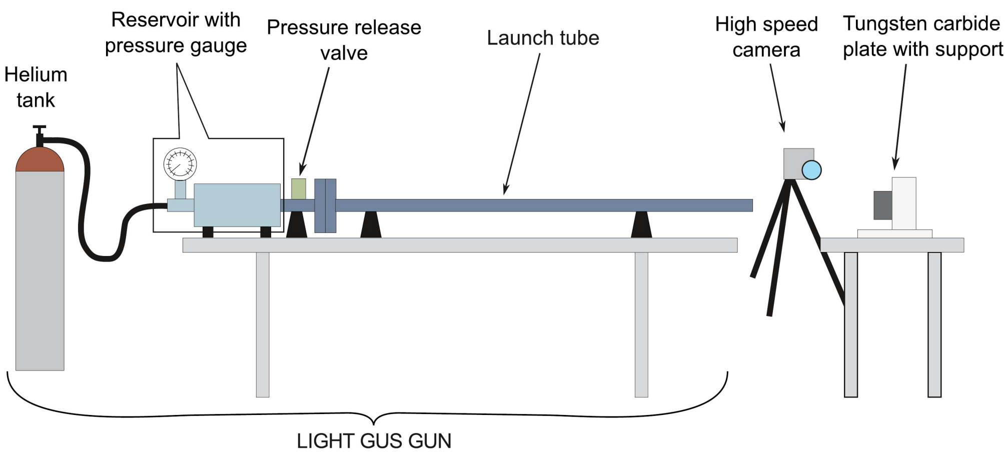

FIG. 6. Schematic of the Taylor DIE setup.

FIG. 7. Specimens recovered after the Taylor DIE.

Calculations were performed on the basis of relationships (4.17) and (4.18) using experimental data. The discrete values of these calculations for some selected values of the velocity V_0 are listed in Table 1 and shown as a graph in Fig. 8.

Table 1. Experimental data and values of the dynamic yield stress for annealed copper (Cu-ETP).

V_0 [m/s]	X [mm]	L_1 [mm]	σ_{sd} [MPa] Eq. (4.17)	σ_{sd} [MPa] TAYLOR Eq. (4.18)
68	1.80	43.25	24	61
125	1.40	37.92	81	91
146	1.10	35.72	110	96
180	0.90	32.73	166	112
214	0.89	29.85	234	133

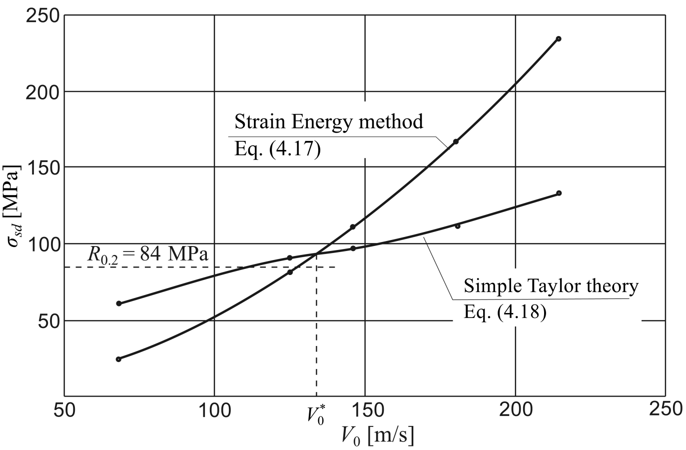

FIG. 8. Variation of the dynamic yield stress *versus* impact velocity for annealed copper (Cu-ETP).

Figure 8 presents large differences between the values of σ_{sd} calculated by means of the formulae (4.17) and (4.18) which exceed 50%. HAWKYARD *et al.* [4, 5] and KOLSKY and DOUCH [16] have obtained similar results when using energy methods.

In addition, from Fig. 8 it follows that for selected value of $V_0 = V_0^* \approx 135$ m/s the difference between $\sigma_{sd\,(4.17)}$ and $\sigma_{sd\,(4.18)}$ is equal to zero. Subsequently with an increase of the magnitude $|V_0 - V^*|$ the difference $|\sigma_{sd\,(4.17)} - \sigma_{sd\,(4.18)}|$ also increases in both directions and it exceeds 50%.

The quantities $\sigma_{sd\,(4.17)}$ and $\sigma_{sd\,(4.18)}$ for $V_0 = V^*$ represent different magnitude. A σ_{sd} (4.17 V_0^*) signifies value of the dynamic yield stress in deformed portion of the copper rod whose length is: $h_2 \frac{L(a-V_0^*)}{(a_0+a_1)} = 5$ mm long. By contrast, σ_{sd} (4.18 V_0^*) signifies a mean value of the dynamic yield stress of the deformed copper sample $L_1(V_0) - X(V_0^*) \approx 37$ mm long.

One ought to also take notice that for small impact velocity the dynamic yield stress of annealed copper (Cu-ETP) is smaller than the static yield stress (Fig. 8). This result can be surprising, because for majority of metals the dynamic yield stress is greater than the static one ($\sigma_{sd} > \sigma_s$). However some metals behave in an opposite way [11, 17–19], i.e. $\sigma_{sd} < \sigma_s$; for example that is how the annealed copper behaves at moderate magnitude of the impact velocity ([13], p. 103, Table 5). The Taylor theory gives a simple result (Fig. 8), as might be expected.

6. Conclusion

In accordance with the theory of Taylor DIE each and every successive fragment of the deformed portion of the rod is suddenly stopped and struck by an undeformed part of the rod whose length and velocity decrease during the impact test. The velocity of the undeformed part of the rod decreases in a continuous way from $V = V_0$ to $V = 0$ during the impact process. The Taylor formula (4.18) contains the final values of the geometrical parameters of the deformed rod after the impact test, namely, X and L_1. Each deformed element of the rod gives an increment to the values of these parameters during the Taylor DIE. For this reason the Taylor formula (4.18) determines the mean value of dynamic yield stress not for the given impact velocity $V = V_0$, but for the average velocity contained in the range $0 \leq V \leq V_0$. Taylor's impact theory does not define the value of this average velocity. Besides, the Taylor formula (4.18) is based on a rate-independent rigid ideal-plastic material and does not allow a large increase of the strain rate in the final stage of deforming of the rod during the impact test (about 10^4 1/s). In addition, the formula (4.18) does not fulfil a dynamic condition across the plastic wave front. This is contradictory to physics of shock waves.

On the contrary formula (4.17) defines the value of the dynamic yield stress of the rod material at given impact velocity, i.e. $v = V_0$ at the initial stage of deforming of the rod. In period t_s (equal to about over a dozen percent μs) the strain-rate of the rod material has a quasistatic form (Fig. 2). This specific distribution of strain rate along the axis of the deformed sample during the initial stage of the Taylor DIE is used in the presented method. In this method, behaviour of the material of the initial deformed portion of the rod is described by means of an elastic-plastic model with linear strain hardening without an influence of the strain rate on the dynamic parameters of the rod material. Thus a simple algebraic formula for determining dynamic yield stress of metals loaded by the Tylor DIE has been derived.

On the basis of the results presented in this paper one can confirm that Taylor's theory fails to provide reliable dynamic yield stress estimates, especially for material sensitive to strain rate, such as annealed copper under the impact loading.

The proposed method is based on the theory of weak shock waves [14] and the variation of the internal energy and temperature in the striking rod is neglected. For this reason thermal softening of the material and failure [20] of the rod were not considered (see Fig. 7).

References

1. Taylor G.I., *The use of flat-ended projectiles for determining dynamic yield stress I. Theoretical considerations*, Proceedings of the Royal Society of London, Series A, **194**(1038): 289–299, 1948, doi: 10.1098/rspa.1948.0081.

2. Whiffin A.C., *The use of flat-ended projectiles for determining dynamic yield stress II. Tests on various metallic materials*, Proceedings of the Royal Society of London, Series A, **194**(1038): 300–322, 1948 doi: 10.1098/rspa.1948.0082.

3. Lee E.H., Tupper S.J., *Analysis of plastic deformation in a steel cylinder striking a rigid target*, Journal of Applied Mechanics, Transactions of ASME, **21**: 63–70, 1954.

4. Hawkyard J.B., Eaton D., Johnson W., *The mean dynamic yield strength of copper and low carbon steel at elevated temperatures from measurements of the mushrooming of flat-ended projectiles*, International Journal of Mechanical Sciences, **10**(12): 929–948, 1968, doi: 10.1016/0020-7403(68)90048-9.

5. Hawkyard J.B., *A theory for the mushrooming of flat-ended projectiles impinging on a flat rigid anvil, using energy consideration*, International Journal of Mechanical Sciences, **11**(3): 313–333 1969, doi: 10.1016/0020-7403(69)90049-6.

6. Jones S.E., Muadlin P.J., Foster J.C., *An engineering analysis of plastic wave propagation in the Taylor test*, International Journal of Impact Engineering, **19**(2): 95–106, 1997, doi: 10.1016/S0734-743X(96)00020-6.

7. Lu G., Wang B., Zhang T., *Taylor impact test for ductile porous materials – Part 1: theory*, International Journal of Impact Engineering, **25**(10): 981–991, 2001, doi: 10.1016/S0734-743X(01)00027-6.

8. Wang B., Zhang T., Lu G., *Taylor impact test for ductile porous materials – Part 2: experiments*, International Journal of Impact Engineering, **28**(5): 499–511, 2003, doi: 10.1016/S0734-743X(02)00105-7.

9. Zhang E., Wang B., *On the compressive behavior of sintered porous coppers with low to medium porosities – Part 1: Experimental study*, International Journal of Mechanical Sciences, **47**(4–5): 744–756, 2005, doi: 10.1016/j.ijmecsci.2004.12.011.

10. Włodarczyk E., Sarzyński M., *Analysis of dynamic parameters in a metal cylindrical rod striking a rigid target*, Journal of Theoretical and Applied Mechanics (JTAM), **51**(4): 847–857, 2013.

11. Janiszewski J., *Engineering materials testing in conditions of dynamic load* [in Polish], WAT, Warsaw 2012.

12. Włodarczyk E., Sarzyński M., *Experimental analysis of density and compressive strain of porous metal with the use of Taylor test*, Archives of Mechanics, **66**(4): 245–256, 2014.

13. Rakhmatulin H.A., Demianov Yu.A., *Strength under intensive momentary loads* [in Russian], Moscow 1961.

14. Cristescu N., *Dynamic plasticity*, North – Holland Publishing Company, Amsterdam 1967.

15. Włodarczyk E., *Terminal ballistics of bullets* [in Polish], WAT, Warsaw 2006.

16. Kolsky H., Douch L.S., *Experimental studies in plastic wave propagation*, Journal of the Mechanics and Physics of Solids, **10**(3): 195–223, 1962, doi: 10.1016/0022-5096(62)90038-8.

17. Zukas J.A., Nicholas T., Swift H.F., Greszczuk L.B., Curran D.R., *Impact dynamics*, Wiley, New York 1982.

18. Higashi K., Mukai T., Kaizu K., Tsuchida S., Tanimura S., *The microstructural evolution during deformation under several strain rates in a commercial 5182 aluminum alloy*, Journal de Physique IV France, **01**(C3): C3-347–C3-352, 1991, doi: 10.1051/jp4:1991350.

19. Zukas J.A., *High Velocity Impact Dynamics*, Wiley, New York 1990.

20. Julien R., Jankowiak T., Rusinek A., Wood P., *Taylor's test technique for dynamic characterization of materials: application to brass*, Experimental Techniques, **40**(1): 347–355, 2016.

Received February 2, 2016; accepted version May 19, 2017.